Highlights of DØ Physics

DØ Note 2539

Editor: John D. Hobbs
Physics Group Contributors: Andrew Brandt, Herb Greenlee,
Wyatt Merritt, Paul Quintas, Andrzej Zieminski

April 14, 1995

Abstract

This note is the basis of the DØ contribution to the 1995 *Fermilab Annual Program Review*. It contains a summary of some recent DØ results from all physics groups.

The DØ collaboration consists of approximately 430 physicists from 44 institutions in 9 countries. The DØ research program encompasses a wide variety of basic phenomena. The program can be divided into five major areas – top physics, new particle searches, W and Z physics providing precision tests of the Standard Model, b-quark studies, and studies of the strong interaction QCD. The following list of recent papers illustrates this clearly:

1. "First Generation Leptoquark Search in $p\bar{p}$ Collisions at $\sqrt{s} = 1.8$ TeV", S. Abachi *et al.* (DØ Collaboration), Phys. Rev. Lett. 72, 965 (1994).

2. "Search for the Top Quark in $p\bar{p}$ Collisions at $\sqrt{s} = 1.8$ TeV", S. Abachi *et al.* (DØ Collaboration), Phys. Rev. Lett. 72, 2138 (1994).

3. "Rapidity Gaps between Jets in $p\bar{p}$ Collisions at $\sqrt{s} = 1.8$ TeV", S. Abachi *et al.* (DØ Collaboration), Phys. Rev. Lett. 72, 2332 (1994).

4. "Search for High Mass Top Quark Production in $p\bar{p}$ Collisions at $\sqrt{s} = 1.8$ TeV", S. Abachi *et al.* (DØ Collaboration), Phys. Rev. Lett. **74**, 2422 (1995).

5. "Inclusive μ and b-Quark Production Cross Sections in $p\bar{p}$ Collisions at $\sqrt{s} = 1.8$ TeV", S. Abachi *et al.* (DØ Collaboration), (To be published in Phys. Rev. Lett.).

6. "Measurement of the $ZZ\gamma$ and $Z\gamma\gamma$ Couplings in $p\bar{p}$ Collisions at $\sqrt{s} = 1.8$ TeV", S. Abachi *et al.* (DØ Collaboration), (Submitted to Phys. Rev. Lett.).

7. "Observation of the Top Quark", S. Abachi *et al.* (DØ Collaboration), DØ Collaboration, S. Abachi *et al.*, Phys. Rev. Lett. **74**, 2632 (1995).

8. "Search for W Boson Pair Production in $p\bar{p}$ Collisions at $\sqrt{s} = 1.8$ TeV", S. Abachi *et al.* (DØ Collaboration), (Submitted to Phys. Rev. Lett.).

9. "Search for Squarks and Gluinos in $p\bar{p}$ Collisions at $\sqrt{s} = 1.8$ TeV", S. Abachi *et al.* (DØ Collaboration), (Submitted to Phys. Rev. Lett.).

Additional papers are nearing completion. These include measurements of the W and Z cross sections, the $WW\gamma$ couplings, the W mass, α_s using $W+$ Jets events, and results from a Z' search. This section contains a survey of some recent results and future plans for each of the five physics areas.

1 Top Quark Physics

The top quark is the sixth and final quark required by the Standard Model particle theory. (Other quarks may exist, but they would be by definition "non-standard.") The search for and study of the Standard Model top quark has been and remains an extremely active area of research in DØ. The increasing luminosity delivered by the Fermilab Tevatron has permitted the search to be carried out with ever greater sensitivity. Since the beginning of 1994, DØ has published three papers on the search for the top quark. The last of these, which was submitted simultaneously with a similar paper by CDF, represents the successful culmination of a long effort to find the top quark. This DØ paper concludes that "...we have observed the top quark and measure its mass to be 199^{+19}_{-21} (stat.) ± 22 (syst.) GeV/c^2 and its production cross section to be 6.4 ± 2.2 pb." With this result, the discovery phase is over, and we will begin to study the properties of the top quark.

The top quark search in DØ assumes that the top quark is produced in pairs by the strong interaction, and decays 100% of the time into a W boson and a b quark, as required by the Standard Model. Top quark events are divided into different categories depending on how the W bosons decay. The main searches take place in modes where both W's decay into leptons (the dilepton modes: $e\mu$, ee, and $\mu\mu$) or where just one W decays leptonically (the single-lepton modes: e and μ). The single-lepton modes are further categorized on the basis of soft-muon-tagging of the b quarks or "topological" event selection. In addition to the dilepton and single-lepton modes, the top quark pair may decay into τ leptons (with at least one τ decaying into hadrons) or only into quarks. In all modes, final state quarks are observed as jets and neutrinos are observed as missing transverse energy ($\not\!\!E_{\rm T}$).

The main areas of research in top quark physics in DØ are as follows:

1. Conventional searches in the dilepton and single-lepton modes.

2. Mass analysis in the dilepton and single-lepton modes.

3. Multivariate searches in the dilepton and single-lepton modes.

4. Searches for top decays involving hadronically decaying τ's.

5. Search for top in the all-quark (also called all-jets) decay mode.

6. Search for top quarks produced singly by the weak interaction.

So far, most of the published and presented results have been in the area of the first two items in this list. However, groups in DØ are working on all of the above topics.

1.1 The Conventional Counting Experiment

In the conventional top quark search, one attempts to isolate a nearly pure sample of top quark events by means of one- and two-dimensional cuts on a limited number of variables. All of the published top quark search results are based on conventional searches in the dilepton and single-lepton decay modes. The following table (Table 1) gives the latest result of the conventional counting experiment, where we observed 17 events with an expected

Table 1: Efficiency $\times$ branching fraction ($\varepsilon \times \mathcal{B}$) using standard event selection and the expected number of top quark events ($\langle N \rangle$) in the seven channels, based on the central theoretical $t\bar{t}$ production cross section of Laenen *et al.*, for four top masses. Also given are the expected background, integrated luminosity, and the number of observed events in each channel.

m_t (GeV/c^2)		$e\mu$ + jets	ee + jets	$\mu\mu$ + jets	e + jets	μ + jets	e + jets/μ	μ + jets/μ	ALL
140	$\varepsilon \times \mathcal{B}(\%)$	0.17 ± 0.02	0.11 ± 0.02	0.06 ± 0.01	0.50 ± 0.10	0.33 ± 0.08	0.36 ± 0.07	0.20 ± 0.05	
	$\langle N \rangle$	1.36 ± 0.21	1.04 ± 0.19	0.46 ± 0.08	4.05 ± 0.94	2.47 ± 0.68	2.93 ± 0.68	1.48 ± 0.42	13.80 ± 2.07
160	$\varepsilon \times \mathcal{B}(\%)$	0.24 ± 0.02	0.15 ± 0.02	0.09 ± 0.02	0.80 ± 0.10	0.57 ± 0.13	0.50 ± 0.08	0.25 ± 0.06	
	$\langle N \rangle$	0.94 ± 0.13	0.69 ± 0.12	0.34 ± 0.07	3.13 ± 0.54	2.04 ± 0.53	1.95 ± 0.39	0.92 ± 0.24	10.01 ± 1.41
180	$\varepsilon \times \mathcal{B}(\%)$	0.28 ± 0.02	0.17 ± 0.02	0.10 ± 0.02	1.20 ± 0.30	0.76 ± 0.17	0.56 ± 0.09	0.35 ± 0.08	
	$\langle N \rangle$	0.57 ± 0.07	0.40 ± 0.07	0.19 ± 0.04	2.42 ± 0.67	1.41 ± 0.36	1.14 ± 0.22	0.64 ± 0.16	6.77 ± 1.09
200	$\varepsilon \times \mathcal{B}(\%)$	0.31 ± 0.02	0.20 ± 0.03	0.11 ± 0.02	1.70 ± 0.20	0.96 ± 0.21	0.74 ± 0.11	0.41 ± 0.08	
	$\langle N \rangle$	0.34 ± 0.04	0.25 ± 0.05	0.11 ± 0.02	1.84 ± 0.31	0.95 ± 0.24	0.81 ± 0.16	0.41 ± 0.10	4.71 ± 0.66
Background		0.12 ± 0.03	0.28 ± 0.14	0.25 ± 0.04	1.22 ± 0.42	0.71 ± 0.28	0.85 ± 0.14	0.36 ± 0.08	3.79 ± 0.55
$\int \mathcal{L}dt$ (pb^{-1})		47.9 ± 5.7	55.7 ± 6.7	44.2 ± 5.3	47.9 ± 5.7	44.2 ± 5.3	47.9 ± 5.7	44.2 ± 5.3	
Data		2	0	1	5	3	3	3	17

background of 3.8 ± 0.6 events. The probability that the 17 observed events arise entirely from a background fluctuation is 2×10^{-6} (equivalent of a 4.6σ standard deviations). The result of the counting experiment is a measurement of a production cross section. Our measured cross section is shown in Fig. 1 as a function of the assumed top quark mass.

A second analysis was performed with less restrictive selection criteria. This gave a sample with considerably larger background contamination than the 17 event sample above. The resulting cross-section is in good agreement with the cross-section from the 17 event sample.

1.2 Mass Analysis

The goal of the mass analysis is the direct measurement of the top quark mass. It is possible to perform mass analyses in either the dilepton or single-lepton decay modes. An example of a dilepton mass analysis was given in last year's program review. Since then the focus of effort has shifted to doing mass analysis in the single-lepton modes. The reasons for this are, first, that unlike the dilepton decay modes it is possible to fully reconstruct single-lepton events, and second, there are many more single-lepton events available for mass fitting.

The mass analysis of $t\bar{t} \to l\nu q\bar{q}'b\bar{b}$ candidate events effectively uses six measured vectors, the lepton momentum, the $\not{E}_T$, and the momenta of four jets as approximations to the true momenta of the lepton, neutrino and four quarks in each each event. These, along with resolution functions and background shapes, are input to a two constraint kinematic fit. The constraints include overall momentum conservation, equality of the reconstructed masses of both top quarks, and the difference between the mass of the reconstructed W's and the W mass. Figure 2 shows the top quark mass distribution of fully reconstructed candidate top quark events for two sets of event selection cuts.

The difficulties in performing this procedure are numerous. First, the component of the neutrino momentum along the beam cannot be measured. Second, the jets in a event are not partons. Third, initial and final state radiation change the mean and shape of

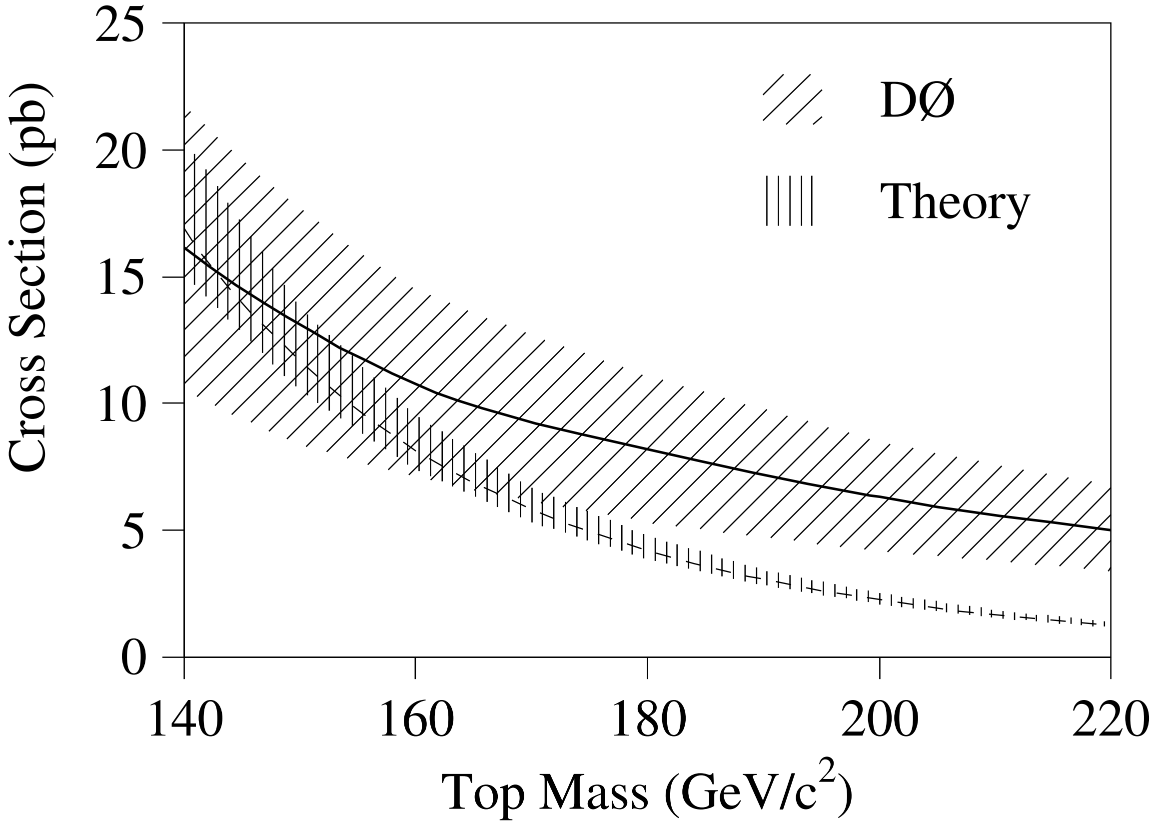

Figure 1: DØ measured $t\bar{t}$ production cross section (solid line with one standard deviation error band) as a function of assumed top quark mass. Also shown is the theoretical cross section curve (dashed line).

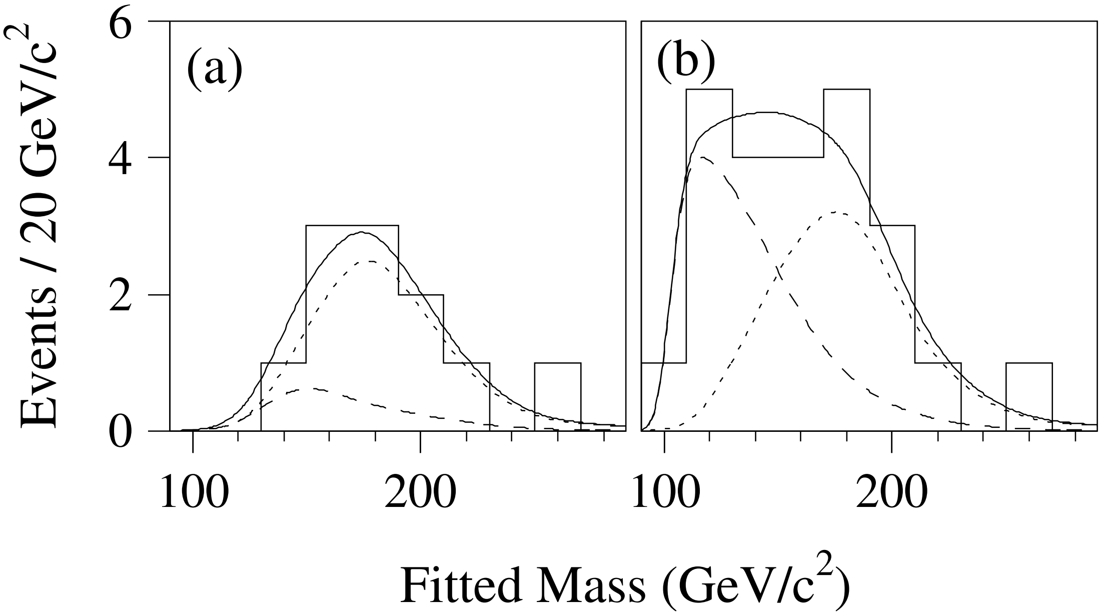

Figure 2: Fitted mass distribution for candidate events (histogram) with the expected mass distribution for 199 GeV/c^2 top quark events (dotted curve), background (dashed curve), and the sum of top and background (solid curve) for (a) standard and (b) loose event selection.

the reconstructed mass distribution, and fourth, the assignment of jets to partons cannot be determined *a priori*. These problems are dealt with by a combination of energy corrections to the jets, the constraints in the fitting process and a calibration procedure. The jet energies are related to parton energies using a p_T-dependent energy correction derived from a combination of data and Monte Carlo. The shift in reconstructed mass caused by energy arising from final state radiation which is found outside the four jets used in the fit is corrected using the calibration procedure. Finally, the appropriate jet assignments are chosen by comparing the χ^2 values returned for each of the possible assignment combinations.

1.3 Multivariate Analyses

Multivariate techniques are an alternative to the conventional cuts method of isolating a nearly pure sample of top quark events. In conventional analyses, one is in practice limited to making one- and two-dimensional cuts. In multivariate analysis, various techniques are used to generate multidimensional cuts for optimal separation of signal and background. Three techniques are currently being studied in DØ: Neural networks, probability density estimation (PDE), and the "H-matrix" (or covariance matrix) technique. The H-matrix technique has been used successfully in DØ for many years to distinguish electron and photon calorimeter clusters from jets. An H-matrix based algorithm for distinguishing hadronic τ decays from jets is currently under development.

In all cases, the goal of the multivariate analysis methods is to improve the signal to background ratio over that which can be obtained using conventional analysis for a given efficiency. Since the top quark statistics will be limited for the forseeable future, multivariate techniques may produce the largest possible sample of top quark events for mass analysis or for other studies. Multivariate techniques may also aid in isolating signals in the more difficult decay modes described in the next section.

1.4 Other Decay Modes

The top decay modes involving τ leptons and the all-quark decay modes are more difficult than the dilepton and single-lepton decay modes due to larger backgrounds. Results on these modes have not yet been published by DØ. However, the Standard Model makes definite predictions on the branching ratios of these decay modes relative to the dilepton and single-lepton decay modes. The measurement of the τ and all-quark decay modes are important for confirming that the massive particle signals observed by DØ are in fact the Standard Model top quark. For example, one way in which the top quark may be non-standard is if it decays some of the time into a charged Higgs boson $H^{\pm}$ instead of a W boson. Unlike the W boson, the charged Higgs decays predominantly into τ leptons rather than e or μ leptons. Therefore, excess τ decays could be evidence for charged Higgs being produced by top decay. The all-quark decay mode has the largest branching ratio of all of the decay modes. It is the only neutrinoless decay mode which makes it potentially useful for mass analysis.

1.5 Single Top Quark Production

In addition to the dominant strong interaction pair production mechanism, top quarks may be produced singly by the weak interaction. Relative to the amount of phase space available, single top production is much weaker than pair production, and the backgrounds are therefore worse. However, single-top events would be very interesting if they could be isolated. The production mechanisms for single top production provide an interesting test of the Standard Model in their own right. The mass analysis of single-top quark events is much more straightforward than the mass analysis of top quark pair events. Another interesting feature of singly produced top quarks is that they are produced polarized, which permits measurements of top quark couplings that can not be made using unpolarized pair-produced top quarks.

2 Results from Searches for New Phenomena

A number of searches for phenomena beyond the Standard Model have been pursued by DØ using the data from Run Ia. These searches are now being extended to include the Run Ib data, and additional topics accessible with the increased luminosity of Run Ib are also under study. These topics are perhaps the most speculative area under study by DØ – any discoveries would significantly change the current standard picture of fundamental interactions.

The range of searches undertaken by DØ has led to:

1. A mass limit on first generation scalar leptoquark. This was the first published Run Ia DØ physics result.

2. A mass limit on the second generation leptoquark.

3. Limits on the masses of squarks and gluinos, within the context of the Minimal Supersymmetric Standard Model (MSSM).

4. Cross section times branching fraction limits on gaugino production in the MSSM context.

5. Limits on the masses of a heavy right-handed W and its associated (heavy) neutrino.

Also completed is a search for indications of compositeness in events with high scalar transverse energy. This will be translated to limits on the compositeness scale soon.

These searches will be extended by additional data from Run Ib. Additional searches for b' quarks, heavy neutral leptons, charged and neutral Higgs particles, massive stable particles, and other exotica are being pursued.

So far, however, DØ has reported only limits – no new phenomena have been seen.

2.1 The First Generation Leptoquark Search

Leptoquarks are hypothetical point-like particles carrying the quantum numbers of both leptons and hadrons. The existence of such objects would point to a merging of the apparently disjoint classes of quarks and leptons.

Leptoquarks would be produced dominantly in pairs and each of the pair decays into a standard, sequential lepton and a quark. Thus, a first generation leptoquark decays into either an electron and a quark or an electron neutrino and a quark.

The search for first generation leptoquarks involves two experimental signatures: 2 electrons + 2 jets, and 1 electron + 2 jets + $\not\!\!E_T$. The backgrounds arising from vector bosons + jets are completely eliminated by the analysis requirements, and the remaining backgrounds from continuum lepton production and jet misidentifications are quite small. The leptoquark mass limit versus the leptoquark branching fraction into electrons is shown in Fig. 3. At a $p\bar{p}$ collider, this search is virtually independent of the unknown leptoquark coupling to leptons and (uud), and is thus quite orthogonal to searches at HERA.

2.2 The Second Generation Leptoquark Search

The second generation leptoquark decays exclusively to muons and muon neutrinos, so the same sort of search as in the previous section can be performed using muons in place of electrons. The limit plot obtained with this search is shown in Fig. 4.

2.3 The Squark/Gluino Search

Among the leading theoretical models which require extensions to the Standard Model are the various super symmetry (SUSY) theories. These theories address the fundamental asymmetry between the fermionic quarks and leptons and the bosonic force carriers by hypothesizing the existance of bosonic quarks and leptons and fermionic force carriers.

The models can be stretched over a very wide phenomenological space and have very few experimental constraints. However, the most constrained of these models are likely to be accessible at the Tevatron. The first DØ search for evidence of super symmetric interactions looks for squarks (the super symmetric partners of quarks) and gluinos (the super symmetric partners of gluons) via their hadronic cascade decays. The signal would have multiple jets and significant $\not{E}_{\mathrm{T}}$, arising from the escape of the weakly interacting, stable, lightest super symmetric particle (LSP) at the end of the decay chains. After strict requirements on the jets and $\not{E}_{\mathrm{T}}$, the background from multijet events with fluctuations in the measured jet energies is negligible, and the number of events seen, and their distribution in $\not{E}_{\mathrm{T}}$, is well predicted by the estimated background from vector bosons + jets. The mass limit contour in the squark-gluino mass plane is shown in Fig. 5.

2.4 The Wino/Zino Search via Trilepton Final States

The other SUSY states likely to be accessible at the Tevatron are the winos and zinos (also called charginos and neutralinos). A very clean, low-background signature of three leptons + $\not{E}_T$ exists for pair production of $\tilde{W}_1 + \tilde{Z}_2$. Since the daughter leptons are of relatively low momentum for the mass range to be investigated in Run Ia (from the LEP limit of 47 GeV/c^2 to roughly 60 GeV), the total detection efficiency is rather low. This is illustrated by the transverse momentum (p_T) distributions of signal leptons and $\not{E}_{\mathrm{T}}$. (Fig. 6). There are currently no broad-based limits placed on the masses from DØ , but the cross section times branching fraction into trileptons, shown in Fig. 7, does limit some specialized models. This search particularly will benefit from the more efficient triggering and increased luminosity in Run Ib.

2.5 The Search for Compositeness via Events with Large Scalar E_T

Although the quarks and leptons are assumed in the Standard Model to be point-like objects, it is natural to test this assumption whereever possible. One method of testing this assumption is to search for evidence of compositeness in events with high energy flow in the plane perpendicular to the beam. This is a direct analogy with the Rutherford scattering

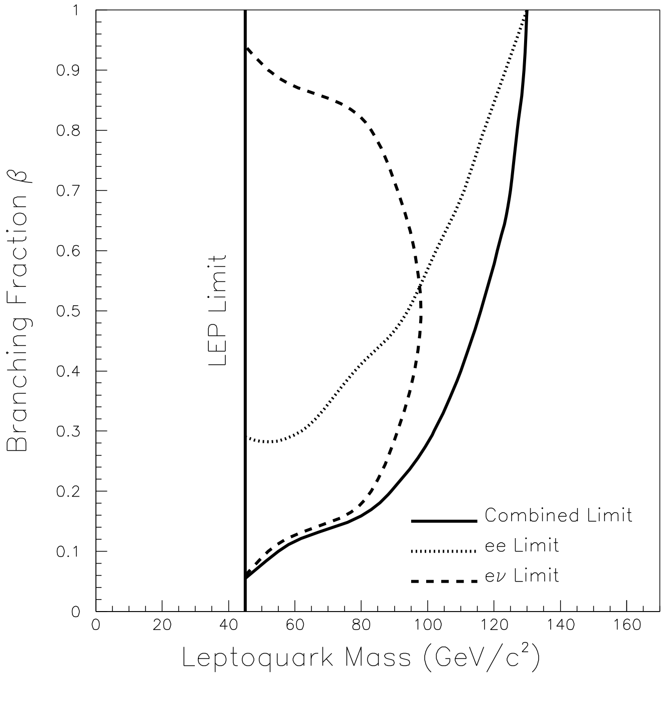

Figure 3: Mass limits for a first generation leptoquark.

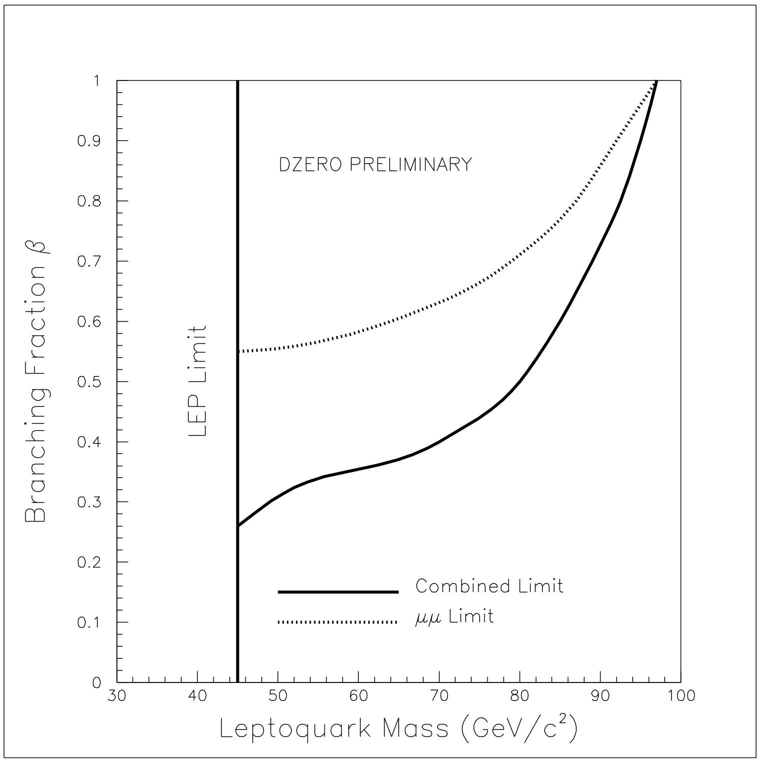

Figure 4: Mass limits for a second generation leptoquark.

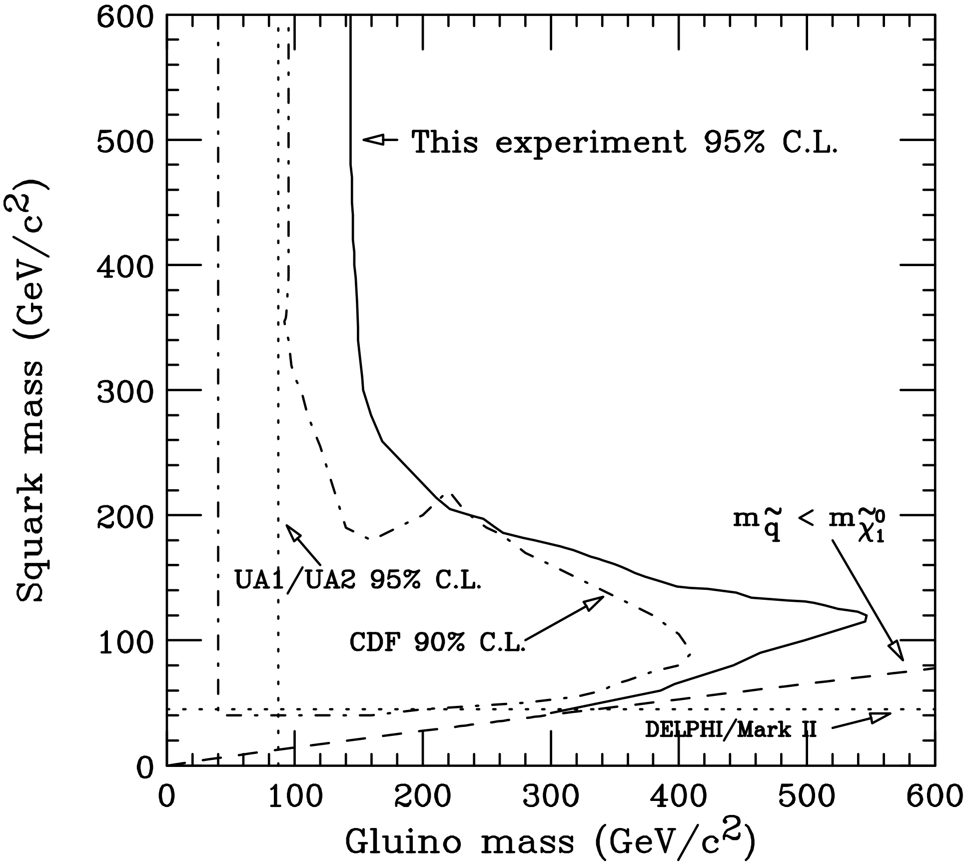

Figure 5: Mass limits for squarks and gluinos.

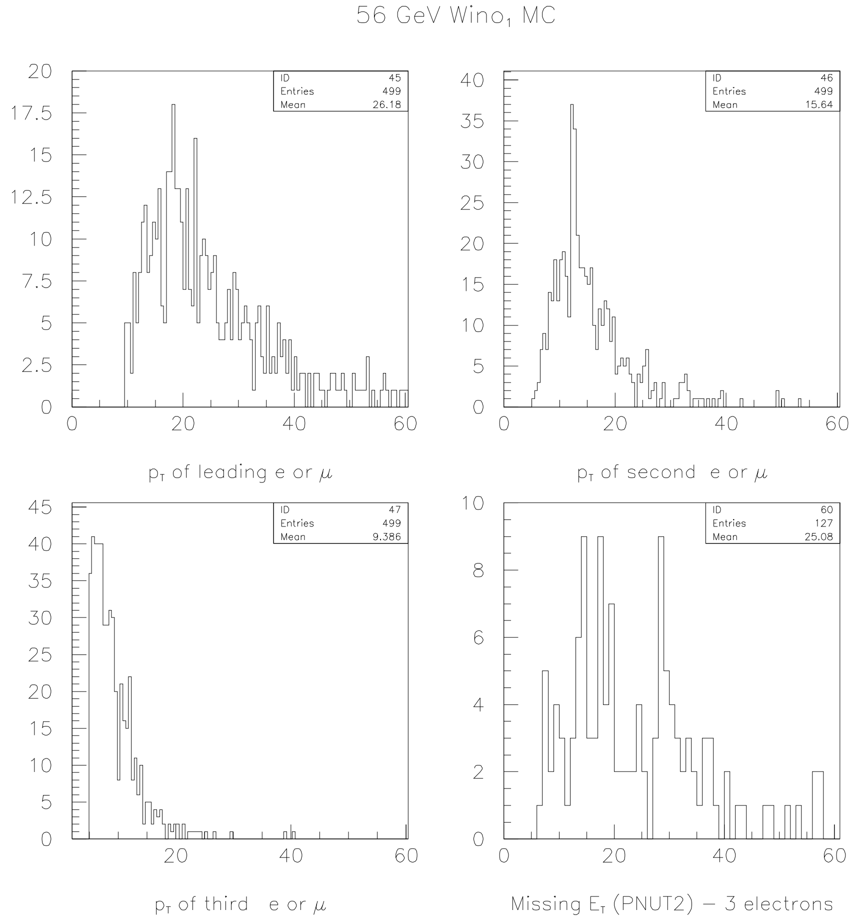

Figure 6: Monte Carlo estimates of the p_T and $\not\!\!E_{\rm T}$ distributions for leptons from $\tilde{W}_1$ and $\tilde{Z}_2$ decays in the mass range accessible with Run Ia data.

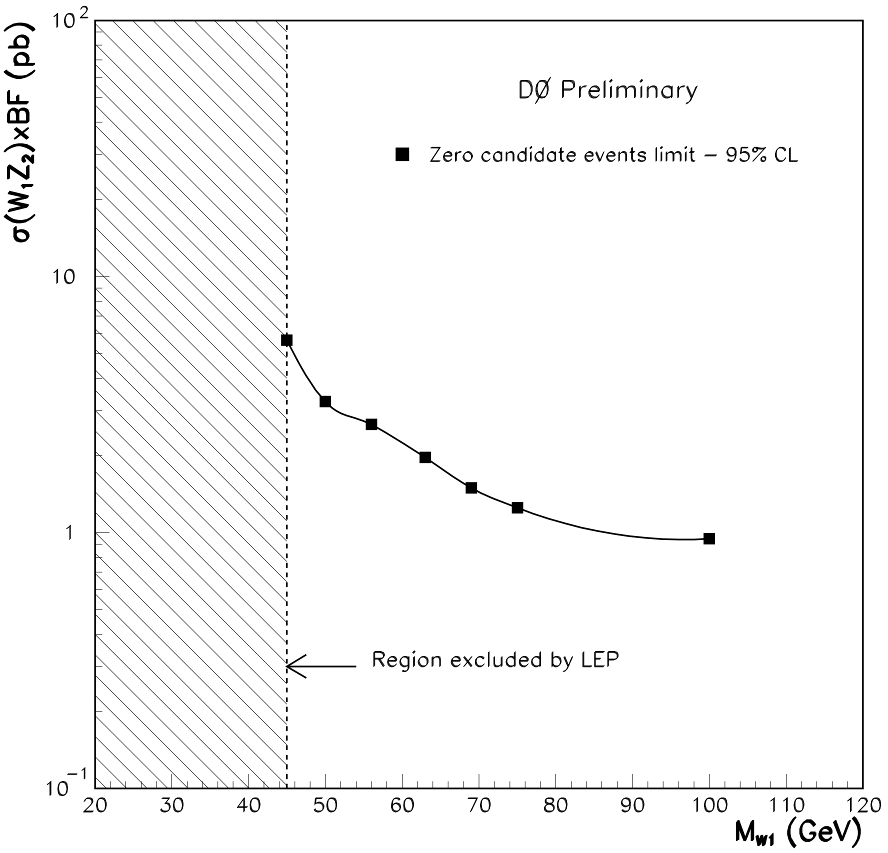

Figure 7: Cross-section times branching ratio limit for $\tilde{W}_1 + \tilde{Z}_2 \rightarrow (l_1 l_2 l_3)$.

experiments performed at the turn of century which lead to the discovery of the atomic nucleus.

A search for such events has been carried out. No evidence for departure from expected behavior has been seen, and this will soon be converted to a limit on the compositeness scale.

2.6 Summary

In conclusion, the searches completed thus far on Run Ia data have in many cases significantly extended limits on various new phenomena, but unfortunately have not given evidence yet for any effects or particles beyond the Standard Model. Much more remains to be done with these data and with the greatly increased luminosity from Run Ib, and such searches will be extended significantly.

3 Electroweak Physics Results

3.1 W Mass Measurement

The measurement of the W boson mass $M_W$is one of the critical measurements for hadron collider experiments. This precision measurement, combined with the Z boson mass, width and decay asymmetries from the e^+e^- collider experiments, overconstrains the Standard Model. In addition, the value of the W mass, combined with the top quark mass will begin to place constraints on the Higgs mass.

DØ has measured the W boson mass using electron events; the signal is a high p_T electron with large $\not{E}_{\mathrm{T}}$ arising from the non-interacting neutrino. Since the neutrino's momentum along the incoming beam direction is not measured, the transverse mass

$$M_T^W = \sqrt{2p_T^l p_T^\nu(1 - cos\phi_{l,\nu})} \tag{1}$$

is the experimentally reconstructed quantity. Here $\phi_{l,\nu}$ is the azimuthal angle between the lepton and the neutrino direction. M_W is measured by fitting the data M_T^W spectrum with a set of M_T^W template distributions generated from Monte Carlo simulation with different input masses. The best fit to the M_T^W spectrum is shown in Fig. 9.

Crucial to this measurement is the understanding of the hadronic and electromagnetic energy scales. These effects are studied using the $Z \to e^+e^-$ events. The kinematics of the Z and W decays are similar, but since both decay leptons are observed in Z events, the requirement that the transverse momentum of the dilepton pair balance the recoiling hadronic system fixes the hadronic energy scale.

The energy scale of the DØ calorimeter is set by the measurement of the Z mass. The linearity of the calibration is checked making use of the range of electron energies from Z decays, and the π^0 (from $\pi^0 \to \gamma\gamma$ in which both photons produce eletroncs from photoconversion) and $J/\Psi \to e^+e^-$ peaks. For the first method, the Z mass can be fit as a function of the factor $f = 2(E_1 + E_2)\sin^2(\gamma/2)/M$ where E_1 and E_2 are the energies of the electrons, γ is the opening angle, and M is the invariant mass. Figure 8 shows the fit to this data. The slope consistent with zero implies linearity of the calibration. This information combined with the observed positions of the π^0 and $J/\Psi \to e^+e^-$ mass peaks determines the electromagnetic scale factor and limits the non-linearity.

The preliminary result from the Run Ia data, representing a luminosity of 14 pb^{-1}, from a sample of 4817 events in the central calorimeter, is

$$M_W = 79.86 \pm 0.16(stat) \pm 0.17(syst) \pm 0.26(scale). \tag{2}$$

Systematic studies are in progress, and a final result with reduced errors is expected soon.

3.2 W and Z Production Cross-sections

The production cross-sections of the W and Z bosons are measured by detecting the bosons through their decays into electrons or muons,

$$\begin{aligned} \sigma Br(W) &\equiv \sigma(\mathrm{p}\bar{\mathrm{p}} \to W) \cdot Br(W \to l\nu), \\ \sigma Br(Z) &\equiv \sigma(\mathrm{p}\bar{\mathrm{p}} \to Z) \cdot Br(Z \to l^+l^-). \end{aligned}$$

The ratio of these quantities, combined with LEP measurements of the Z widths and Standard Model calculations of the W partial width to leptons, can be used to derive the total width of the W boson, Γ_W.

$$\begin{aligned} R &= \frac{\sigma Br(W)}{\sigma Br(Z)} \\ &= \frac{\sigma(\mathrm{p}\bar{p} \to W)}{\sigma(\mathrm{p}\bar{p} \to Z)} \cdot \frac{\Gamma_Z}{\Gamma(Z \to l^+ l^-)} \cdot \frac{\Gamma(W \to l\nu)}{\Gamma_W} \end{aligned}$$

This method gives the most precise measurement of Γ_W. The results from the cross-sections, based on the complete Run Ia data samples, of 12.4 pb^{-1} for electrons and 11.1 pb^{-1} for muons, are summarized below. These numbers will improve soon because of better understanding of the DØ luminosity.

Channel	$\sigma Br(W)$ (nb)	$\sigma Br(Z)$ (nb)	R
DØ e	$2.38 \pm 0.07 \pm 0.29$	$0.220 \pm 0.011 \pm 0.026$	$10.82 \pm 0.41 \pm 0.29$
DØ μ	$2.12 \pm 0.23 \pm 0.25$	$0.180 \pm 0.031 \pm 0.022$	$11.8^{+1.8}_{-1.4} \pm 1.1$
combined			10.90 ± 0.49

The DØ measurement of the W width derived from the combined value for R is

$$\Gamma(W) = 2.044 \pm 0.093(stat + syst)\ GeV. \tag{3}$$

The world average prior to this measurement was 2.08 $\pm$ 0.07 GeV. The agreement of the measured width with the Standard Model prediction, $\Gamma(W) = 2.077 \pm 0.014$, can be used to set limits on non-standard W decay modes. For example, if there were a new quark coupling to the b quark with standard couplings, it would be excluded for masses below 61 GeV at the 95% confidence level.

3.3 Diboson Production and Anomalous Coupling Limits

The trilinear coupling of Electroweak gauge bosons is investigated through studies of production and characteristics of events having pair-produced bosons ($W\gamma$, $Z\gamma$, WW, and WZ). The Standard Model makes exact predictions for these couplings and for the cross section and kinematic distributions in these events. In general, the trilinear couplings arising in the s-channel diagrams interfere with the quark exchange diagrams to give characteristic distributions. Anomalous coupling parameters differ from zero only in extensions to the Standard Model. If they are non-zero, the cross sections will be larger and the kinematic distributions enhanced in the high p_T region. Run Ia provided DØ with a sample of 23 candidate $W\gamma$ events and 6 $Z\gamma$ events in approximately 13.4 pb^{-1} of data. This enabled limits to be set on anomalous couplings.

The distribution of the photon transverse energy, the angular separation of the photon from the decay lepton and the three-body transverse mass of photon, lepton and neutrino from leptonic decays of $W\gamma$ events are shown in Fig. 10a) - c). The pure $U(1)$ electromagnetic coupling of the W boson to the photon is excluded at 80% C.L.

A new topic for the Tevatron experiments is the study of W boson pair production. The accumulated data prior to collider Run Ia did not provide sensitivity to the relatively low cross-section of this process. Using the Run Ia data, DØ found one WW candidate with an expected background of about 1/2 of an event. This topic is especially novel because the $t\bar{t}$ background must be removed. This analysis produced limits on the $WW\gamma$ and WWZ trilinear couplings.

The larger luminosity available in Run Ib will allow detailed studies of the kinematic distributions in $W\gamma$ and $Z\gamma$ events, may permit the first observation of the expected amplitude-zero in the $W-\gamma$ angular distribution. We expect to produce a clear sample of WW events, allowing improved trilinear coupling measurements.

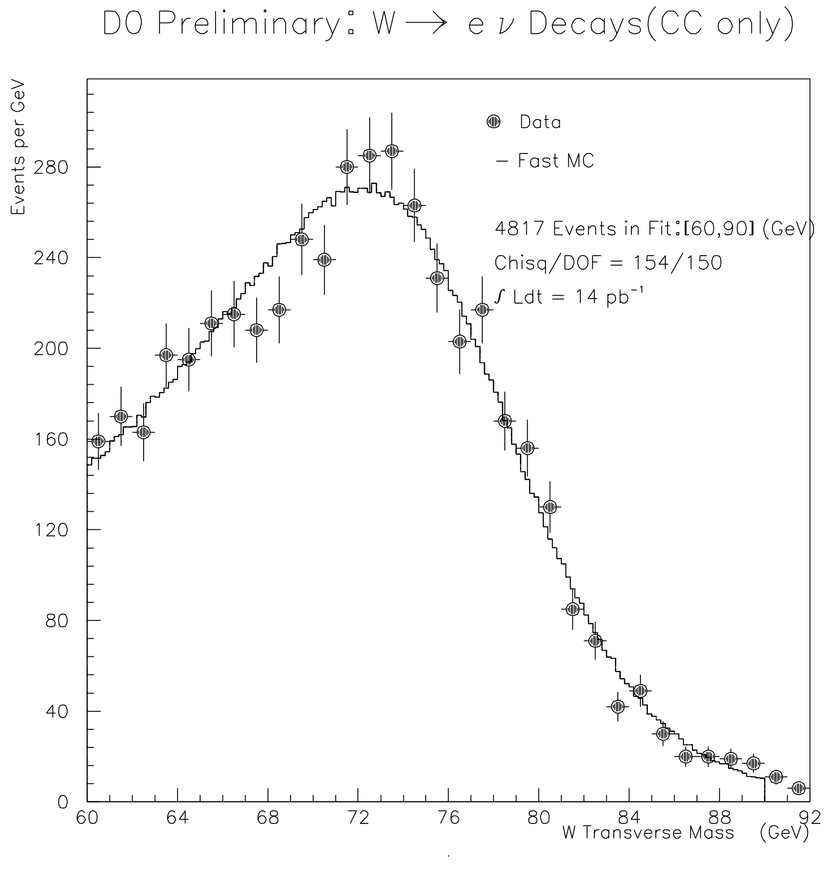

Figure 8: Fit to the W transverse mass for DØ electron data.

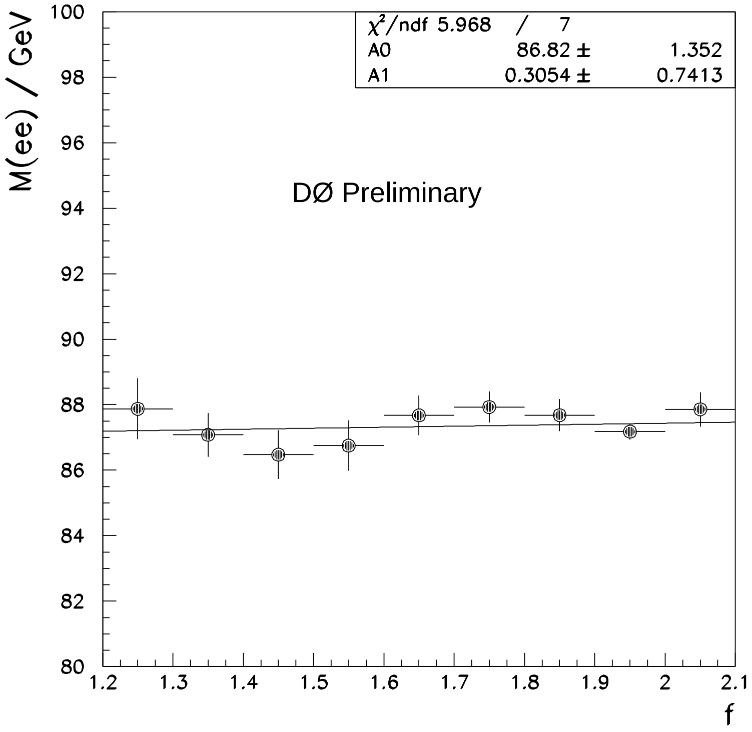

Figure 9: $< M(ee) >$ vs. f (see text) for the $Z \to ee$ sample.

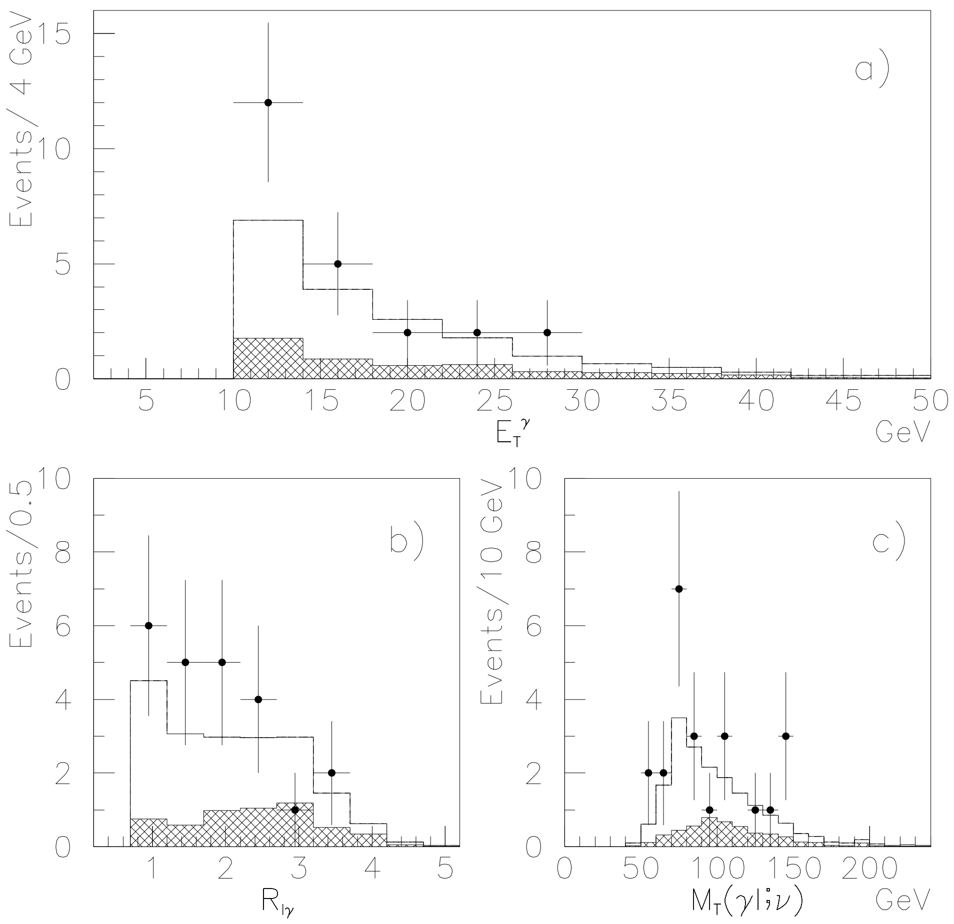

Figure 10: Distribution of (a) E_T^{γ}, (b) $R_{l\gamma}$ and (c) $M_T(\gamma l\nu)$ for the $W(e\nu)\gamma$ and $W(\mu\nu)\gamma$ combined sample. The points are the Run Ia data. The shaded areas represent the estimated background, and the solid histograms are the expected signal from the Standard Model plus the estimated background. $R_{l\gamma}$ is the separation in η, ϕ space between the lepton and the photon.

4 b-Physics at DØ

The study of b-quark production at the Fermilab Tevatron provides an excellent testing ground for the details and procedures of perturbative QCD and will be of interest in coming CP violation studies in the B system. The relatively large b-quark mass implies that theoretical calculations may be more reliable than for other light-quark processes. Furthermore, because b-quark events can be experimentally separated from events without b-quarks, benchmark comparisons to theory in production cross sections and angular correlations can be performed.

Although the DØ detector has been optimized for high p_T physics, its extensive muon detection system combined with triggering capabilities on relatively low-energy muons makes it feasible to study b-physics as well. The DØ muon system provides measurement of muon momentum above 3 GeV/c over a pseudorapidity range $|\eta^\mu| < 3.3$. The thickness of the calorimeter plus iron toroids reduces the hadron punchthrough background to a negligible level of less than 10^{-4} and allows for good identification of muons inside jets.

The hadroproduction of b-quarks has recently been a subject of intense studies, both theoretically and experimentally. The next to leading order (NLO) calculations have been available for some time. The lowest order $b\bar{b}$ production processes (s-channel gluon diagrams or t-channel quark exchange) are rivaled at large p_T by $O(\alpha_s^3)$ diagrams including the t-channel gluon exchanges with subsequent gluon splitting and flavor excitation diagrams. Although earlier UA1 results were in reasonable agreement with NLO QCD calculations at $\sqrt{s} = 630$ GeV, more recent CDF results have tended to be roughly a factor of two higher than the theoretical central values.

The DØ b-physics studies have concentrated on:

1. inclusive b-quark cross sections over a wide rapidity range.

2. production mechanisms for the charmonium (J/Ψ and χ_c) and bottomonium (Υ) states,

3. $b\bar{b}$ correlations,

4. the heavy flavor content of jets.

4.1 Inclusive Cross-section Measurements

The cross section for b-quark production as a function of the minimum transverse momentum of the quark, p_T^{min}, for rapidities less than 1 is shown in Fig. 11. Within errors, our b-quark cross section agrees with that of CDF for inclusive leptons, also shown for comparison. The curves in Fig. 11 represent the NLO QCD predictions. The upper limit on the systematic error in Fig. 11 is computed assuming the renormalization and factorization scale is half the value used for the central value. Thus, the data of both experiments favor smaller values of the renormalization and factorization scale μ.

4.2 Charmonium and Bottomonium Production

A $c\bar{c}$ state is the lightest bound system of quarks for which perturbative QCD is expected to apply. The J/Ψ is of particular significance because of its clean signature through the dilepton decay modes. In high energy $p\bar{p}$ collisions the dominant contributions to the J/Ψ production are expected to come from the lowest order Feynman diagrams with gluon-gluon fusion, either directly into charmonium and a recoiling gluon, or through a $b\bar{b}$ pair followed by a decay $b \rightarrow J/\Psi X$. It has been argued recently that, in addition to the gluon-gluon fusion, the process of gluon fragmentation, i.e. splitting of a virtual gluon into a charmonium state and other partons, is an important source of J/Ψ.

New DØ analyses of the inclusive J/Ψ production confirm the previous CDF cross section measurements. The role of various production mechanisms has been investigated by using vertex information or requiring a third muon which is associated with the non-J/Ψ jet.

Measuring photons associated with J/Ψ's can be used to estimate J/Ψ production from radiative χ_c decays. For example, the χ_c signal of 66 ± 15 events from the run Ia data is shown in Fig. 12. Photons from χ_c decays have energies of order 1 GeV and their reconstruction is a demanding technical test of the DØ electromagnetic calorimeter performance. We estimate that 30 $\pm$ 9% of J/Ψ's with $p_T > 8$ GeV/c and $|\eta| < 0.6$ are due to χ_c production. The Υ production cross section in the central region has been measured as well. Results from both analyses have been presented at the 1995 Moriond Conference.

4.3 Summary

Many more analyses of the existing data are in progress. Inclusive b-quark cross sections will soon become available from events triggered by requiring either two muons or a muon plus a jet. High statistics studies of dimuon and muon-opposite side jet correlations should provide new, more discriminating tests of the QCD calculations. Also, cross section measurements over the full pseudorapidity range ($|\eta| < 3.3$) will probe gluon structure functions at values of x $\approx 10^{-4}$. The DØ capability to study heavy quark production in the forward region are illustrated in Fig. 13 where a dimuon mass spectrum obtained with the forward muon detector for $2.2 < |\eta| < 3.3$ exhibits a clear J/Ψ signal. Evidence of Υ production in this region is in hand as well.

The production of b-quarks at the Tevatron is being actively investigated by the DØ collaboration. With three to five times the data samples from the current collider run in hand, significant improvements in the quality and precision of QCD tests of heavy flavor production are expected.

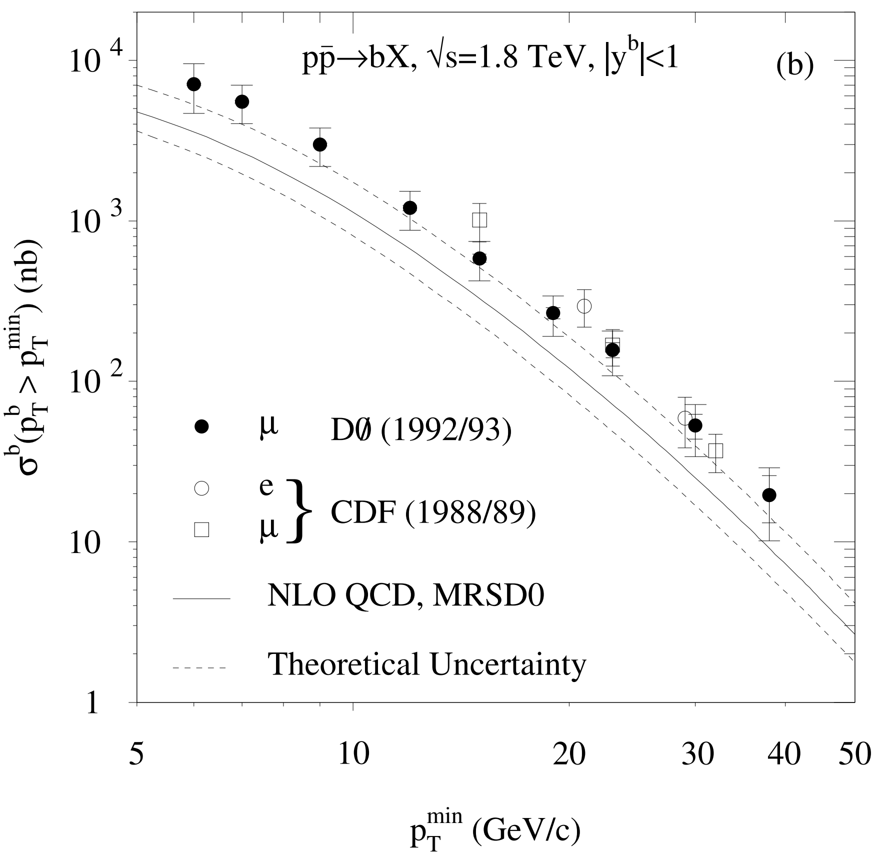

Figure 11: DØ measured b-quark cross-section $d\sigma_b/dp_T$.

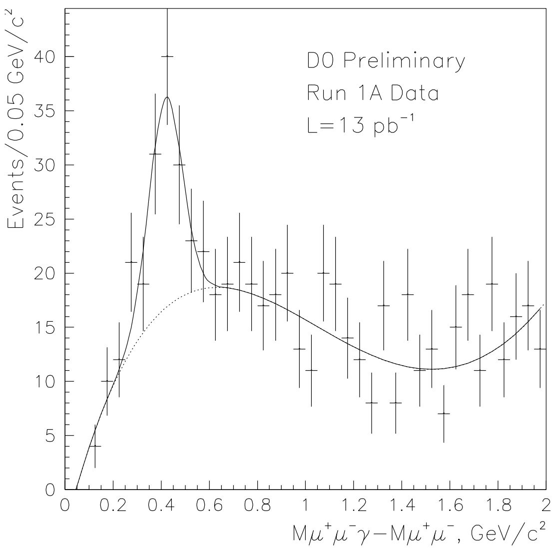

Figure 12: Mass difference $M(\mu\mu\gamma) - M(\mu\mu)$ for the DØ χ_c sample. This shows a clear signal for the decay $\chi_c \rightarrow \gamma J\Psi$.

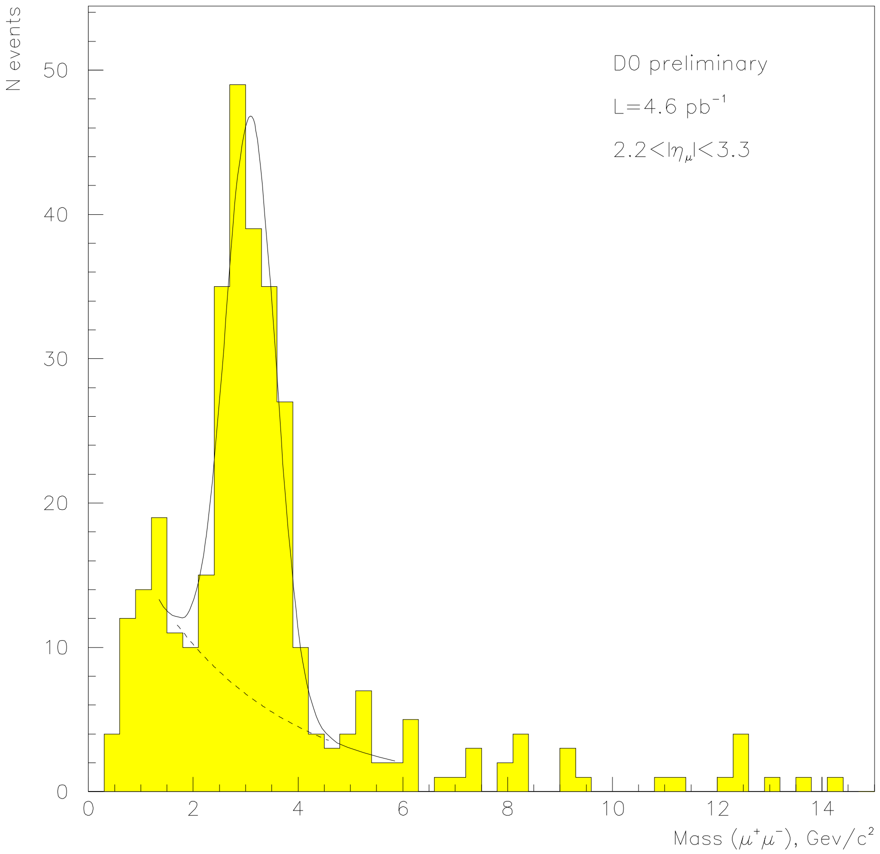

Figure 13: DØ J/Ψ signal from forward $(2.2 < |\eta| < 3.3)$ $\mu^+\mu^-$ events.

5 Strong Interaction Physics

Strong interactions, those responsible for the bound states of nucleii and interactions between quarks, are perhaps the most difficult interactions to characterize using existing models. The difficulty arises from the inherent complexity of the calculations involved. Thus, experimental results are necessary to assess the reliability of various approximation schemes used to make predictions of strong interaction effects. The DØ research in this area covers a wide range of topics, the following of which are discussed here:

1. Jet production
2. Jet shape studies
3. Color coherence
4. Color singlet exchange
5. Dijet decorrelation
6. Inclusive photon production
7. W+Jet production

5.1 Jet Production

Inclusive central jet production has been measured at several center of mass energies and shown to be in excellent agreement with next-to-leading order (NLO) Quantum Chromodynamics (QCD). The hermetic coverage of the DØ detector extends this measurement to forward angles and as such is a rigorous test of QCD near the kinematic limits. As shown in Fig. 14, the DØ data agree within systematic errors (dashed lines) at all pseudorapidities (η) with the NLO calculations (solid lines). This remarkable agreement spans seven orders of magnitude of transverse energy for central jet production and five orders of magnitude for very forward jet production. Since the inclusive cross-section is well described by NLO QCD the DØ analyses can shift now to the measurement of Parton Distribution Functions (PDFs) using correlations between the leading (largest transverse energy) two jets.

Figure 15 shows the η_1 versus η_2 distribution of the two largest transverse energy (E_T) jets for a representative E_T bin. When both jets are at extreme values of rapidity, large and small x regions of the partonic structure functions contribute. These cross sections will provide important input to the global fits used to determine PDFs.

5.2 Jet Shape

Calculations at the parton level, which ignore fragmentation, describe many experimental processes, including inclusive jet and dijet production. We have tested whether NLO partonic QCD predictions can accurately describe the shape of a jet by measuring the transverse energy flow within jets. Jets are divided into ten subcones around the jet axis with radii varying from 0.1 to 1.0 in $\Delta r = \sqrt{\delta\eta^2 + \delta\phi^2} = 0.1$ increments. The jet shape, $\rho(r)$, is defined as the fraction of transverse energy as a function of the subcone radius r. Figure 16 compares the experimentally measured jet shape to NLO predictions (JETRAD) for different renormalization scales, μ, in two different η regions. We see that NLO jet shape predictions are unable to accurately describe the experimentally measured jet shape independent of scale choice.

Future analyses in this area will include comparisons to jet shapes measured at e^+e^- experiments. Preliminary results show jets at e^+e^- experiments to be narrower than jets produced at $p\bar{p}$ colliders. Monte Carlo studies have shown quark jets to be much narrower than gluon jets. Since many more gluon jets are produced at $p\bar{p}$ colliders, this may explain the difference in shape between jets produced in $p\bar{p}$ collisions and in e^+e^- collisions. Investigations of quark and gluon jet differences in the experimental data are underway, and it may be possible to discriminate between quark and gluon jets with reasonable efficiency.

5.3 Color Coherence

Initial and final state color coherence effects in $p\bar{p}$ collisions are studied by measuring spatial correlations between soft and hard jets in multijet events. This analysis thus provides insight into strong-interaction interference between the initial and final state particles. This analysis requires that events have three or more jets with $E_T > 15$ GeV and the leading jet $E_T >$ 120 GeV. Jets were ordered in E_T, and the two leading jets required to be in opposite ϕ hemispheres.

The angular distribution of the softer third jet around the second highest E_T jet in (η, ϕ) space is studied using the angular variable β, measured in the plane defined by the second jet and the beam. The beam directions correspond to $\beta = 0,\ \pi$, and $\beta = \frac{\pi}{2}, \frac{3\pi}{2}$ correspond to the directions perpendicular to the beam. The expectation from initial-final state color interference is that the rate of soft jet emission in the regions $\beta = 0,\ \pi$ will be enhanced with respect to that in the region $\beta = \frac{\pi}{2},\ \frac{3\pi}{2}$.

The data angular distributions are compared with two shower Monte Carlo event generators (ISAJET and HERWIG) that differ in their implementation of color coherence. Figure 17 shows the ratio of the β distributions between data and the two simulations when the second jet is constrained to $|\eta| < 1.5$. ISAJET which uses an independent shower development model (no color coherence effects are included) clearly disagrees with the data, whereas HERWIG, which incorporates color coherence effects by means of an angular ordering approximation of soft gluon radiation, is in qualitative agreement with the data. Complementary analyses are under way to study the color coherence effects of soft gluon radiation by measuring the energy flow patterns in W+jet, γ+jet and jet+jet event samples.

5.4 Color Singlet Exchange

In this analysis we search for strongly interacting color singlet exchange by tagging events with a low multiplicity of particles between jets. Few particles are expected between the leading jets in color singlet events, whereas the presence of a color string connecting the scattered partons in color octet events (gluon exchange) gives rise to a smooth distribution of particles between the leading jets. The color octet multiplicity distribution can be parameterized by a Negative Binomial (NB) distribution. Control samples taken from data and Monte Carlo support this parameterization. An excess of events over the NB fit at low multiplicity signals the presence of color singlet exchange. Figure 18 shows the multiplicity of electromagnetic calorimeter towers with $E_T > 200$ MeV (the DØ method of tagging particles) between the leading jets of an inclusive dijet sample in which the leading jets are separated by at least 4.4 units in rapidity. The large rapidity separation between the leading jets reduces the probability that a color octet event will produce a small number of particles in the region between the jets. There is a clear excess of the data over the NB fit at low multiplicity. The fractional excess in bins of multiplicity 0 to 3 is 1.5 ± 0.2 percent, which is two orders of magnitude above electroweak exchange, and of the same order as rough theoretical estimates of Pomeron exchange by Bjorken and others. This result suggests the presence of a strongly interacting color singlet exchange. Further analyses studying the E_T dependence of color singlet production as well as different species of rapidity gaps are underway.

5.5 Dijet Decorrelation

We study the decorrelation in azimuthal angle between dijets as a function of the pseudorapidity separation between the jets. The variable of interest, $< \cos(\pi - \Delta\phi) >$, is unity for completely correlated (back-to-back) jets and zero for uncorrelated jets. Decorrelation is expected to arise due to soft gluon emissions in the rapidity interval between the jets. The DØ data is compared with a NLO Monte Carlo (JETRAD), a shower Monte Carlo (HERWIG), and the theoretical prediction of Del Duca and Schmidt which is based on BFKL resummation techniques. The comparison is shown in Fig. 19. The data show a significant decorrelation as rapidity increases. HERWIG, which contains a type of resummation in its angular ordered fragmentation process, shows a decorrelation trend similar to the data, while the NLO prediction underestimates the decorrelation and the BFKL prediction overestimates it. Detector effects and the cone size dependence studies are still in progress. Also, an analysis with lower E_T jets allowing a larger rapidity interval is underway.

5.6 Inclusive Photon Production

Direct photons provide an interesting probe of QCD because, unlike jets, they are not subject to final state interactions, they can be relatively unambiguously identified, and their energy is measured accurately. Unfortunately, photons also suffer from a large background due to electromagnetically-fragmenting jets.

A preliminary cross section for the inclusive production of central, isolated direct photons has been measured by DØ and is shown in Fig. 20. Photon candidates with transverse momentum greater than 9 GeV/c and within $|\eta| < 0.9$ were selected by requiring that they be isolated, highly electromagnetic showers in the EM calorimeter, with a shape consistent with test beam electrons, and no track found in the central tracking chambers. The background contribution has been estimated using the longitudinal and transverse shower shape, and by measurement of photon conversions in the drift chambers. After background subtraction, the photon cross section is in good agreement with the next-to-leading order QCD calculation of Owens *et al.*.

5.7 Measurement of α_s in W+jets Events

The running coupling constant α_s is a fundamental expansion parameter in perturbative Quantum-Chromodynamics (QCD) and sets the strength of all strong interactions. The probability of producing jets in association with a W boson is dependent on the value of α_s. The DØ experiment used the ratio of the W+1jet to W+0jets cross sections to determine the value of α_s.

Utilizing 9770 $W \rightarrow e\nu$ candidates from the run Ia, the cross-sections ratio is measured to be $0.065 \pm 0.003(stat) \pm 0.007(syst)$ for $\Delta_R = 0.7$ and jet minimum E_T cutoff (E_T^{min}) of 25 GeV. The recent Next-to-Leading order calculation provides a parameterization of the cross sections of the W+1jet and W+0jets processes in power series of α_s. By equating the experimentally measured ratio with the predictions and solving the equation for α_s, the DØ experiment finds:

$$\alpha_s = 0.123 \pm 0.015 \text{ (combined error)}$$

for CTEQ1M parton distributions at the scale of mass of the W boson (M_W). The dominant uncertainty is due to experimental systematics, particularly jet energy scale. Its size is 0.012. The result is shown in Fig. 21.

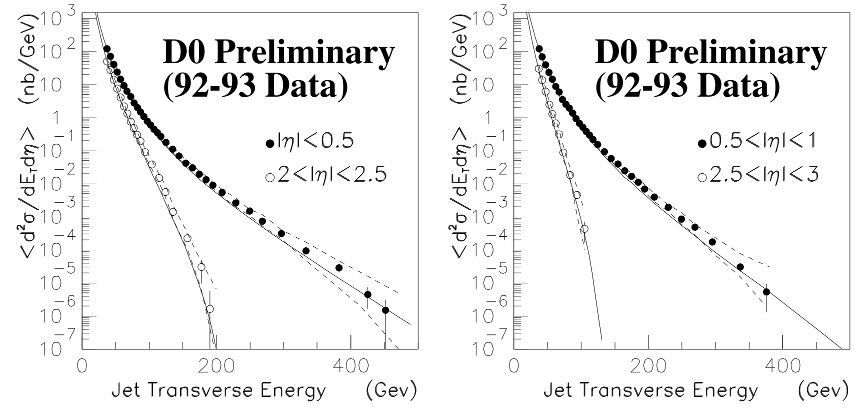

Figure 14: Inclusive jet cross section for several η bins.

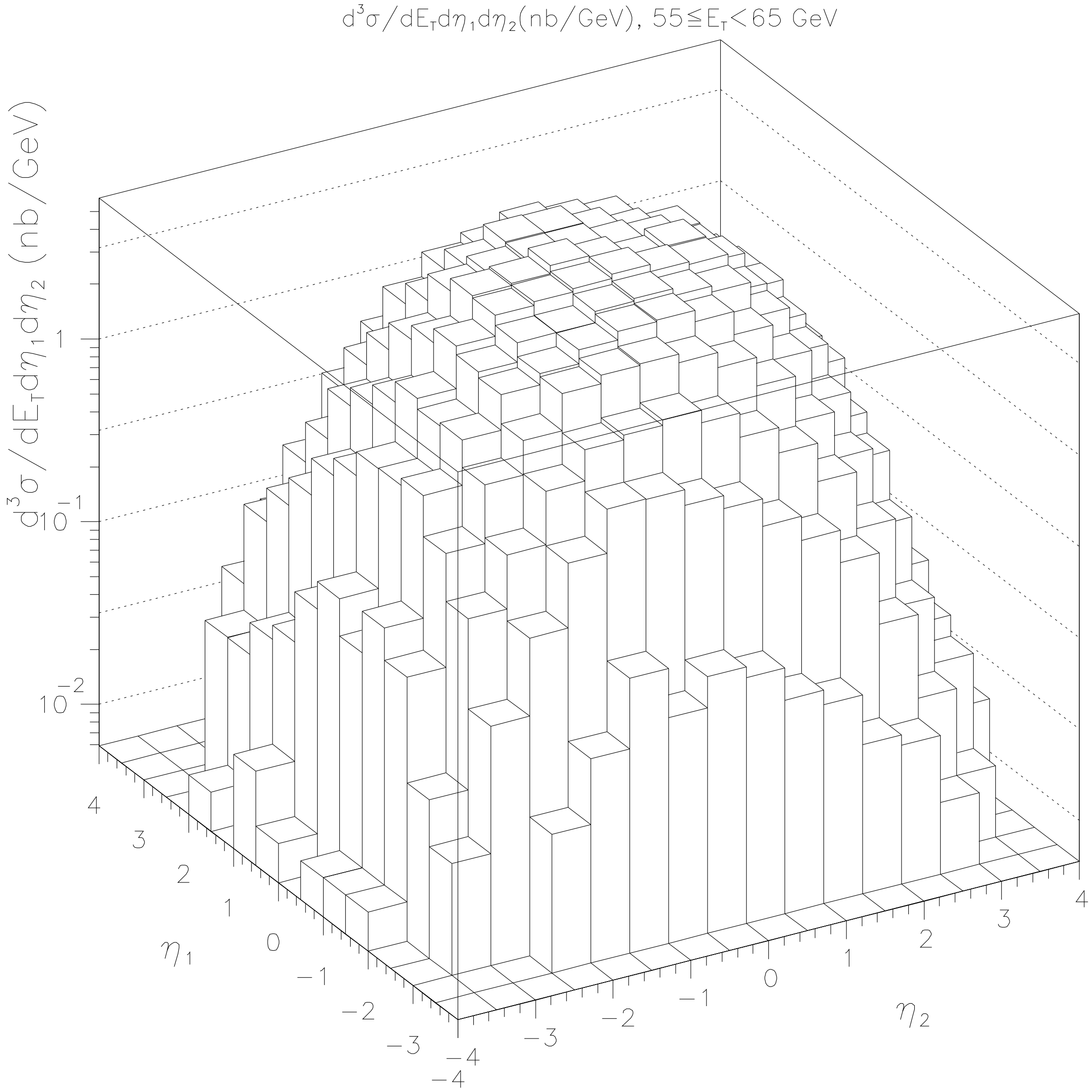

Figure 15: Triple differential cross section as a function of η_1 and η_2 for one E_T bin.

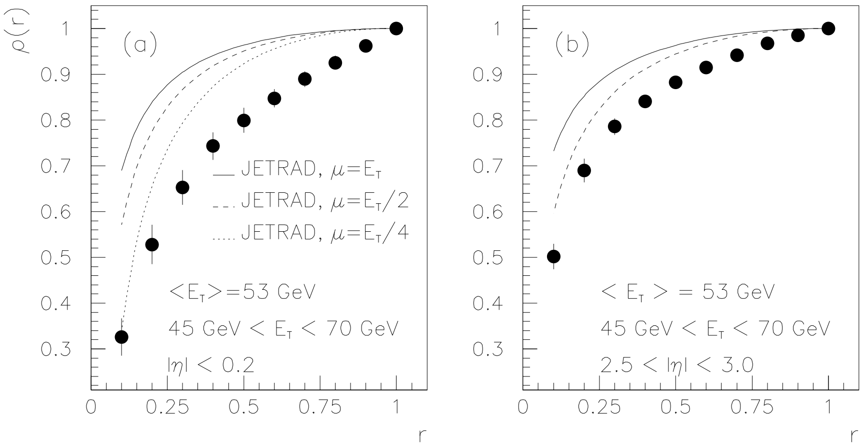

Figure 16: Jet shape for data (dots) and NLO prediction (curves) in central and forward η bins.

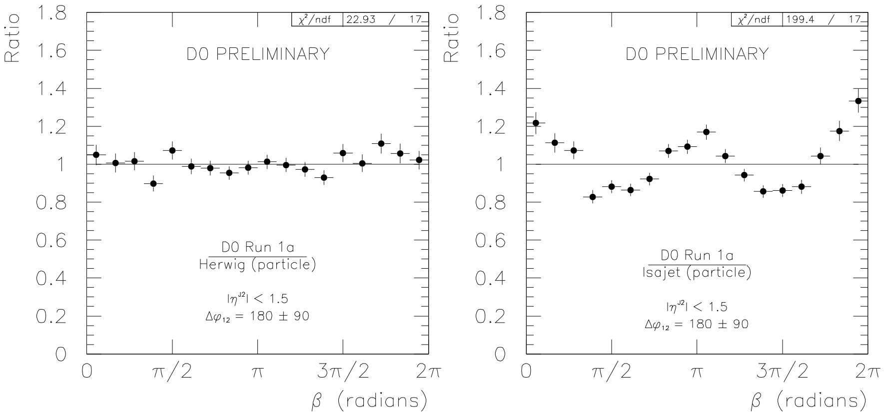

Figure 17: Comparison of the β variable showing location of third jet between data and the HERWIG and ISAJET Monte Carlos.

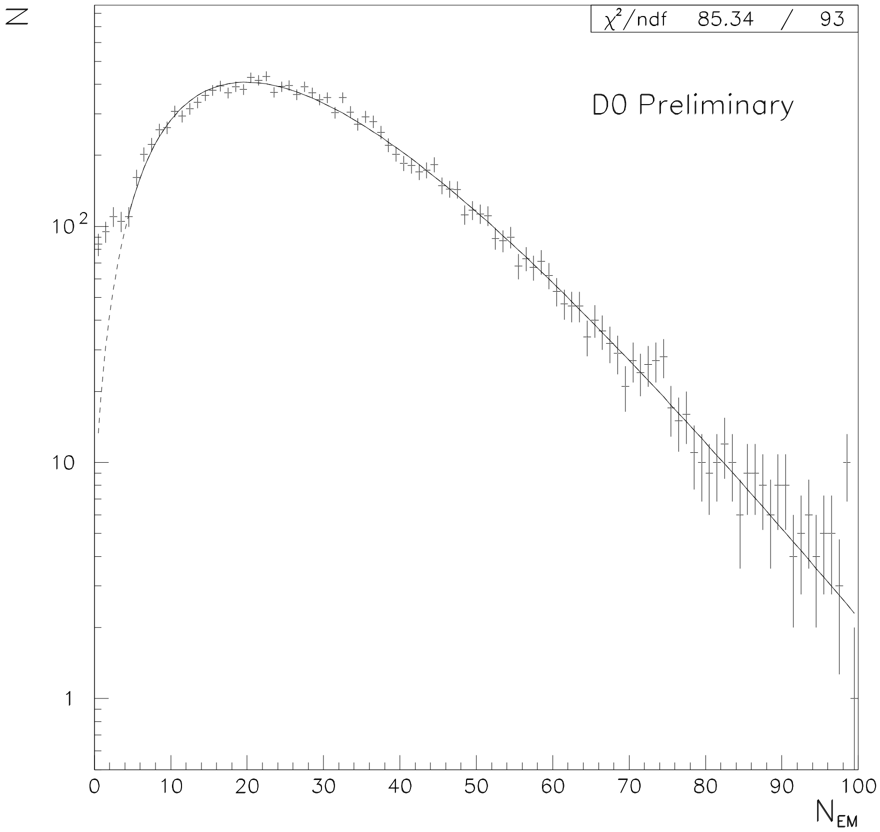

Figure 18: Tower multiplicity between jets with large pseudorapidity separation compared to negative binomial fit.

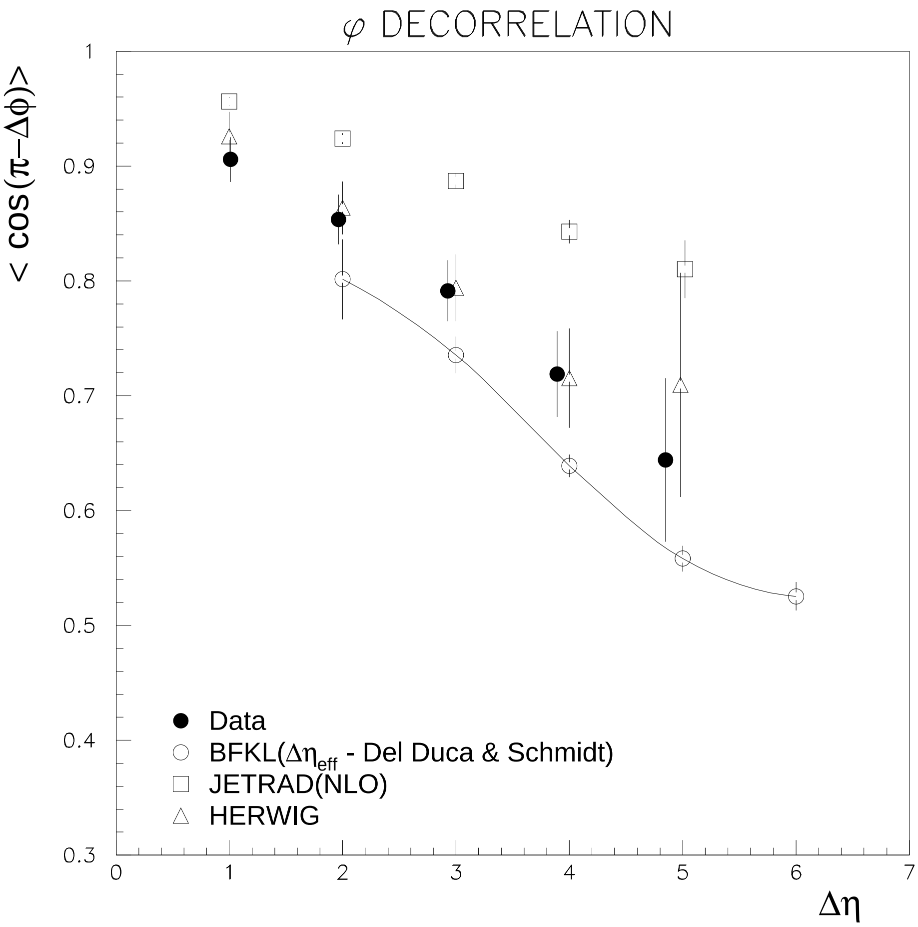

Figure 19: $< \cos(\pi - \Delta\phi) >$ versus $\Delta\eta$ for data compared to JETRAD, HERWIG, and BFKL predictions.

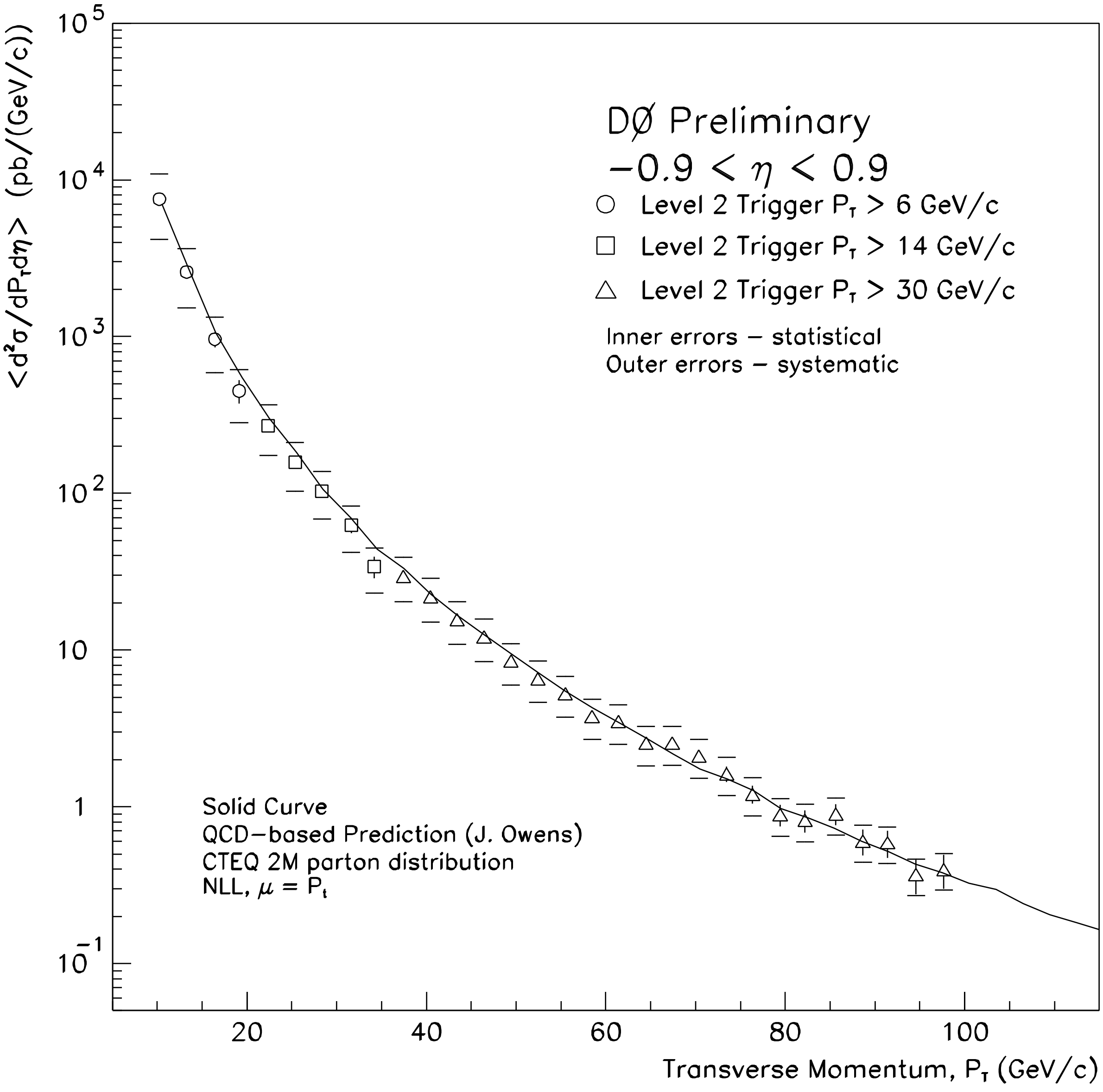

Figure 20: Inclusive photon cross section compared to the QCD prediction.

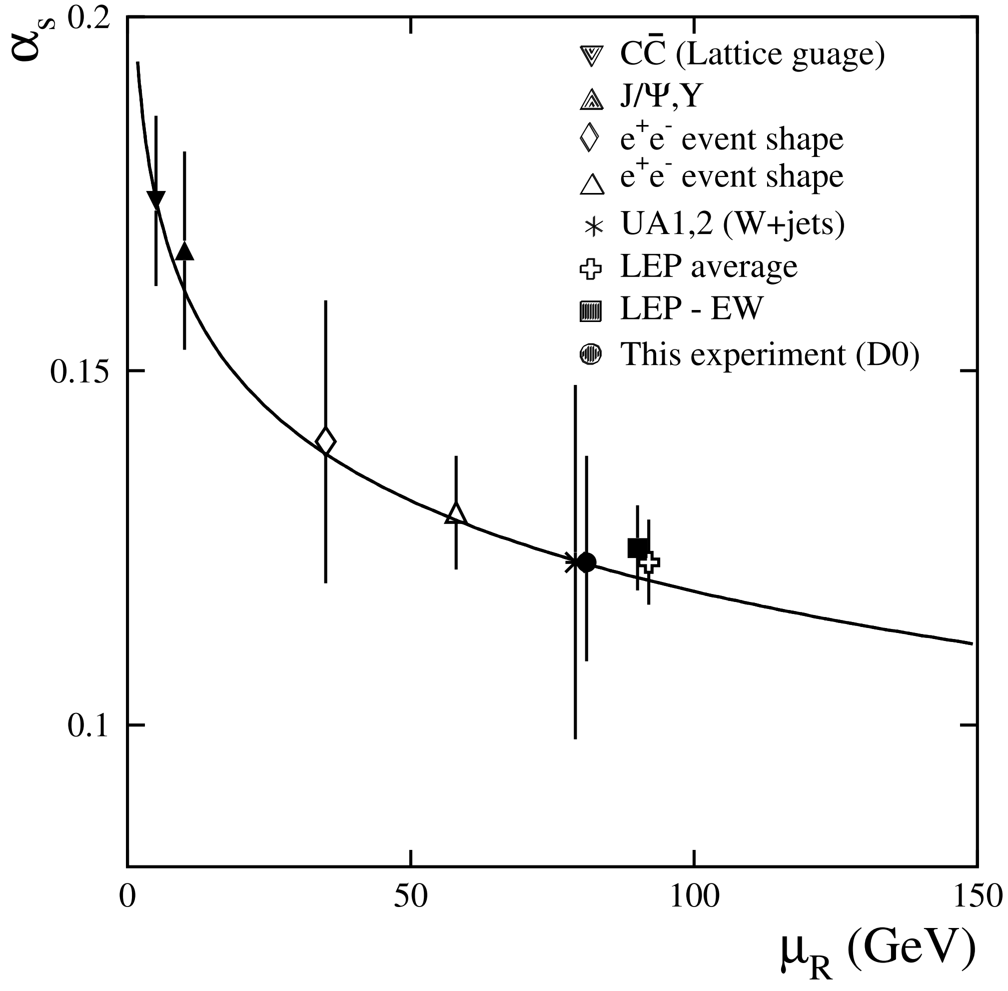

Figure 21: The DØ measurement of α_s shown with other measurements. The horizontal axis is the renormalization scale μ_R.